Vol. 25 • No. 42 • November 11 • 2015

www.afm-journal.de

ADVANCED FUNCTIONAL MATERIALS

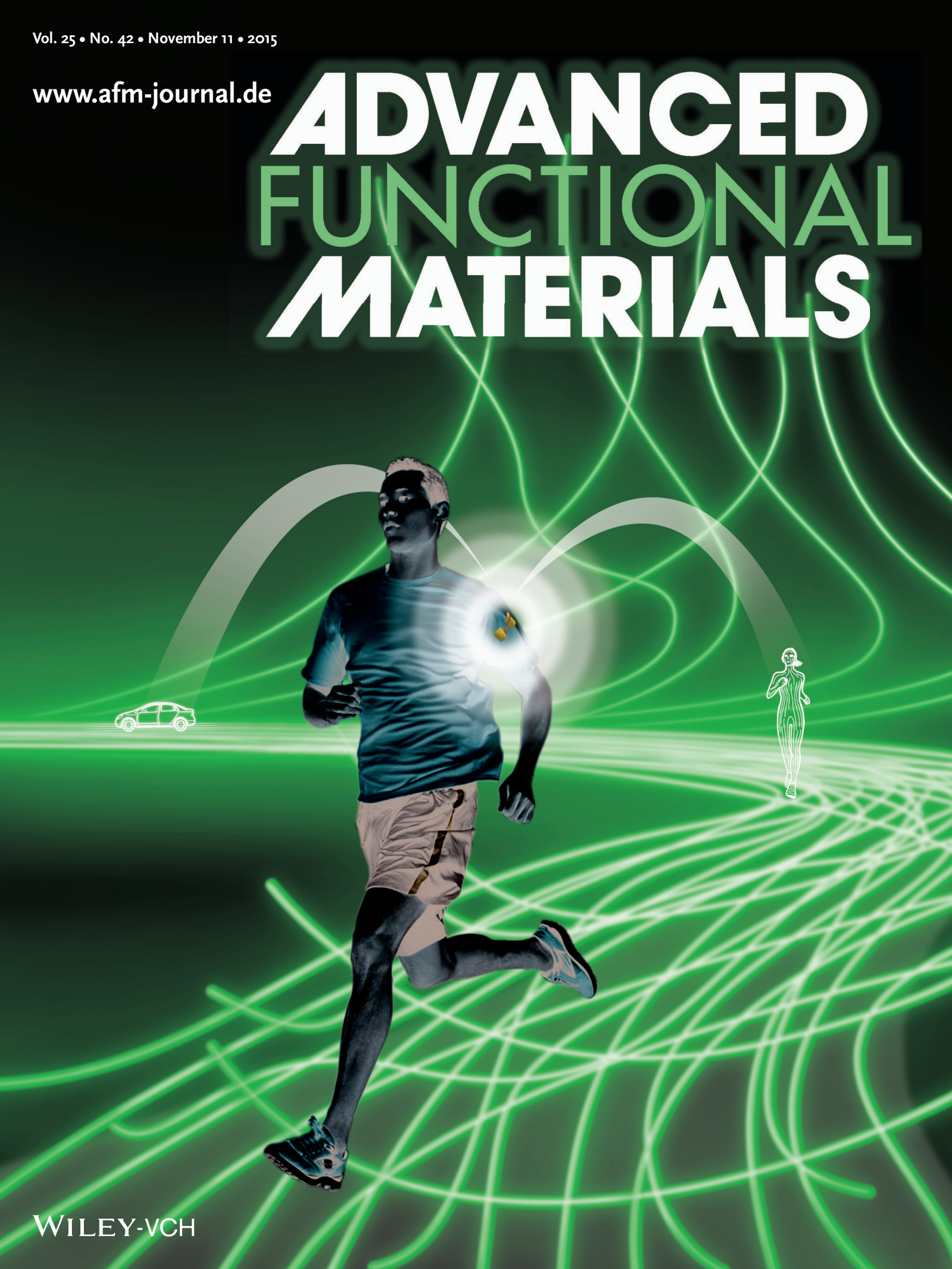

WILEY-VCH

Metal/Polymer Based Stretchable Antenna for Constant Frequency Far-Field Communication in Wearable Electronics

Aftab M. Hussain, Farhan A. Ghaffar, Sung I. Park, John A. Rogers, Atif Shamim,* and Muhammad M. Hussain**

Body integrated wearable electronics can be used for advanced health monitoring, security, and wellness. Due to the complex, asymmetric surface of human body and atypical motion such as stretching in elbow, finger joints, wrist, knee, ankle, etc. electronics integrated to body need to be physically flexible, conforming, and stretchable. In that context, state-of-the-art electronics are unusable due to their bulky, rigid, and brittle framework. Therefore, it is critical to develop stretchable electronics which can physically stretch to absorb the strain associated with body movements. While research in stretchable electronics has started to gain momentum, a stretchable antenna which can perform far-field communications and can operate at constant frequency, such that physical shape modulation will not compromise its functionality, is yet to be realized. Here, a stretchable antenna is shown, using a low-cost metal (copper) on flexible polymeric platform, which functions at constant frequency of 2.45 GHz, for far-field applications. While mounted on a stretchable fabric worn by a human subject, the fabricated antenna communicated at a distance of 80 m with 1.25 mW transmitted power. This work shows an integration strategy from compact antenna design to its practical experimentation for enhanced data communication capability in future generation wearable electronics.

1. Introduction

Flexible and stretchable electronics offer opportunities for a world of wearable electronics. These gadgets can be used for myriad applications such as advanced healthcare,[1–5] monitoring of body's vital signs,[6–10] in situ drug delivery,[11,12] implantable electrodes for brain machine interface etc.[13] Although flexible and non-stretchable electronics can be useful for applications on arbitrarily shaped static surfaces, applications on flexing body parts (elbow, finger joints, wrist, knee, ankle, etc.) require the electronics to be stretchable so as to absorb the strains associated with the movement, thus making stretchability an important aspect of this next generation of electronics. These new age electronic systems require sophisticated data handling and processing capabilities, in addition to being flexible, stretchable, and conformal for their implementation on complex 3D structures. Furthermore, constant data transmission through an integrated communication system is critical. This data communication will enable applications such as wearable healthcare devices that can communicate a user's vital signs to a smart phone and receive instructions for corrective action in real-time. This real-time processing and data storage can eliminate the need for large memory arrays to be integrated with the wearable healthcare monitoring devices, and promises to open new doors for advanced health applications such as a completely body integrated sensor/actuator network. The challenge, in this case, is to build a fully integrated system of sensors, actuators, data processing elements and far-field communication systems on a platform that is both flexible and stretchable. In this paper, we focus on a wearable far-field communication system.

For a communication system to be wearable, all its components have to be made on a flexible and stretchable platform. While the transistors used in RF circuits can be made flexible and stretchable using several techniques demonstrated earlier,[14–17] the main component of the communication circuit, the antenna for far-field communication, is still a challenge. Antenna being a radiative element with a strong dependence on the wavelength of the signal and the shape of the mounting

A. M. Hussain, Prof. M. M. Hussain
Integrated Nanotechnology Lab
CEMSE Division
King Abdullah University of Science and Technology (KAUST)
Thuwal 23955-6900, Saudi Arabia
E-mail: muhammadmustafa.hussain@kaust.edu.sa

F. A. Ghaffar, Prof. A. Shamim
IMAPCT Lab
CEMSE Division, King Abdullah University of Science and Technology (KAUST)
Thuwal 23955-6900, Saudi Arabia
E-mail: atif.shamim@kaust.edu.sa

Dr. S. I. Park, Prof. J. A. Rogers
Department of Materials Science and Engineering
Chemistry, Mechanical Science and Engineering
Electrical and Computer Engineering
Beckman Institute for Advanced Science and Technology
and Frederick Seitz Materials Research Laboratory
University of Illinois at Urbana–Champaign
Urbana, IL 61801, USA
E-mail: jrogers@illinois.edu

DOI: 10.1002/adfm.201503277

© 2015 WILEY-VCH Verlag GmbH & Co. KGaA, Weinheim

platform must be thoroughly investigated for its performance in such applications. There have been several exciting works showcasing a stretchable antenna in the past.[18–22] These systems radiate at different resonant frequencies due to a change in length of the antenna on elongation. Although this can be an interesting property for tunable frequency applications, it is undesirable for the typical single frequency transmit-receive operation. Hence, to complement these systems, we report a stretchable and wearable antenna that can provide a single frequency operation while flexing or stretching. This antenna has been fabricated using a metal/polymer bilayer process and the stretchability is imparted using a lateral spring structure. The key reason the antenna needed to be fabricated as a metal/polymer bilayer is that standalone metal thin films are very malleable, and deform plastically under application of stress. Hence, a metal thin film lateral spring structure cannot be used as a stretchable antenna, since it will only be able to undergo one stretch cycle. The polymer backing provides the restoration force which helps the spring return to its original shape after the release of the applied lateral force.

2. Stretchability Analysis

The metal used to fabricate the antenna was copper (Cu), since it is a common, low-cost metal with excellent conductivity and is compatible with the CMOS fabrication process. Since copper is inherently unstretchable,[23] we adopted a twisted helical spring design to make copper stretchable. Copper has been coupled with a polymer, polyimide (PI), to provide structural support as well as insulation to the antenna. One of the major concerns in designing a stretchable antenna with a metal thin film is the cracking of the metal thin film upon application of stress. This problem can be observed when a metal is deposited on a stretchable polymer base, and the polymer is stretched. This phenomenon was verified by argon (Ar) sputtering a 600 nm layer of copper on a stretchable PDMS base. The copper strip (**Figure 1**a) had an end-to-end resistance of 6 Ω under no strain. However, even with a relatively small lateral strain of 7%, the end-to-end resistance went out of the limit of the measuring instrument (>20 MΩ). This happens due to the cracking of the metal surface as shown in Figure 1a.

This problem was overcome by designing the antenna in such a way that it twists out-of-plane to relieve the stress. This design is based on a twisted helical spring structure. The basic lateral spring structure has been demonstrated in the past for stretchable interconnect applications.[24–30] In this work, we investigate its application as a stretchable antenna. The stretching mechanism of this design is shown in Figure 1b using a simple paper model. The spring elongates in the lateral direction by twisting out of plane at particular points. The paper model is used to demonstrate the stretching mechanism since this out-of-plane twisting (allowing detachment from the host substrate) is clearly visible in the macro-sized model. For a unit cell shown in Figure 1b, the twisting occurs at four points. At each point, the twist causes a 180° phase shift in the plane of the spring. Hence, after two twists, the spring plane is again normal (or aligned back) to the original direction. This is depicted using two different colors, blue and white. The blue plane is normal to the original direction after two twist points (at the center of the spring), and at the end, after four twist points. This elongated lateral spring structure can be approximated as a 3D spiral shown in Figure 1c. The twist points, highlighted with the dotted squares and the colors of the planes have been kept the same for resemblance. The pitch of this spiral (P) is the final length of the elongated spring, and hence will give us the stretchability of a lateral spring structure. Now, the initial circumference (C) of the lateral spring has been twisted into the length of the 3D spiral in Figure 1c. The spiral can be easily described in a cylindrical coordinate system with a constant radial coordinate, and varying θ and z coordinates. For a given pitch P, the theta coordinate goes from 0 to 2π. Hence, the z coordinate can be considered as a function of theta as

$$z = \frac{P\theta}{2\pi} \tag{1}$$

Hence, the 3D spiral is the locus of the point $(r,\theta, P\theta/2\pi)$. This general point can be converted into the Cartesian coordinate system using a simple conversion as $(r\cos\theta, r\sin\theta, P\theta/2\pi)$. For a small change, $d\theta$, in theta, the change in the other coordinates can be obtained. This change can be used to calculate the distance between the two points as

$$dL = \sqrt{(dx)^2 + (dy)^2 + (dz)^2} \tag{2}$$

$$dL = \sqrt{(dr\cos\theta)^2 + (dr\sin\theta)^2 + \left(d\left(\frac{P\theta}{2\pi}\right)\right)^2} \tag{3}$$

$$dL = \sqrt{(r\sin\theta)^2(d\theta)^2 + (r\cos\theta)^2(d\theta)^2 + \left(\left(\frac{P}{2\pi}\right)\right)^2(d\theta)^2} \tag{4}$$

$$dL = \sqrt{r^2 + \left(\left(\frac{P}{2\pi}\right)\right)^2}\, d\theta \tag{5}$$

The integration of this distance over the complete rotations should give the circumference of the original lateral spring. In general, if the lateral spring has n twist points, the total length is given by

$$C = \int_0^{n\pi} \sqrt{r^2 + \left(\left(\frac{P}{2\pi}\right)\right)^2}\, d\theta \tag{6}$$

$$C = n\sqrt{(\pi r)^2 + \left(\frac{P}{2}\right)^2} \tag{7}$$

Further, the diameter of the 3D spiral is the width of the original lateral spring (w). Hence, the pitch can be expressed in terms of the known parameters as

$$P^2 = \left(\frac{2C}{n}\right)^2 - (\pi w)^2 \tag{8}$$

© 2015 WILEY-VCH Verlag GmbH & Co. KGaA, Weinheim

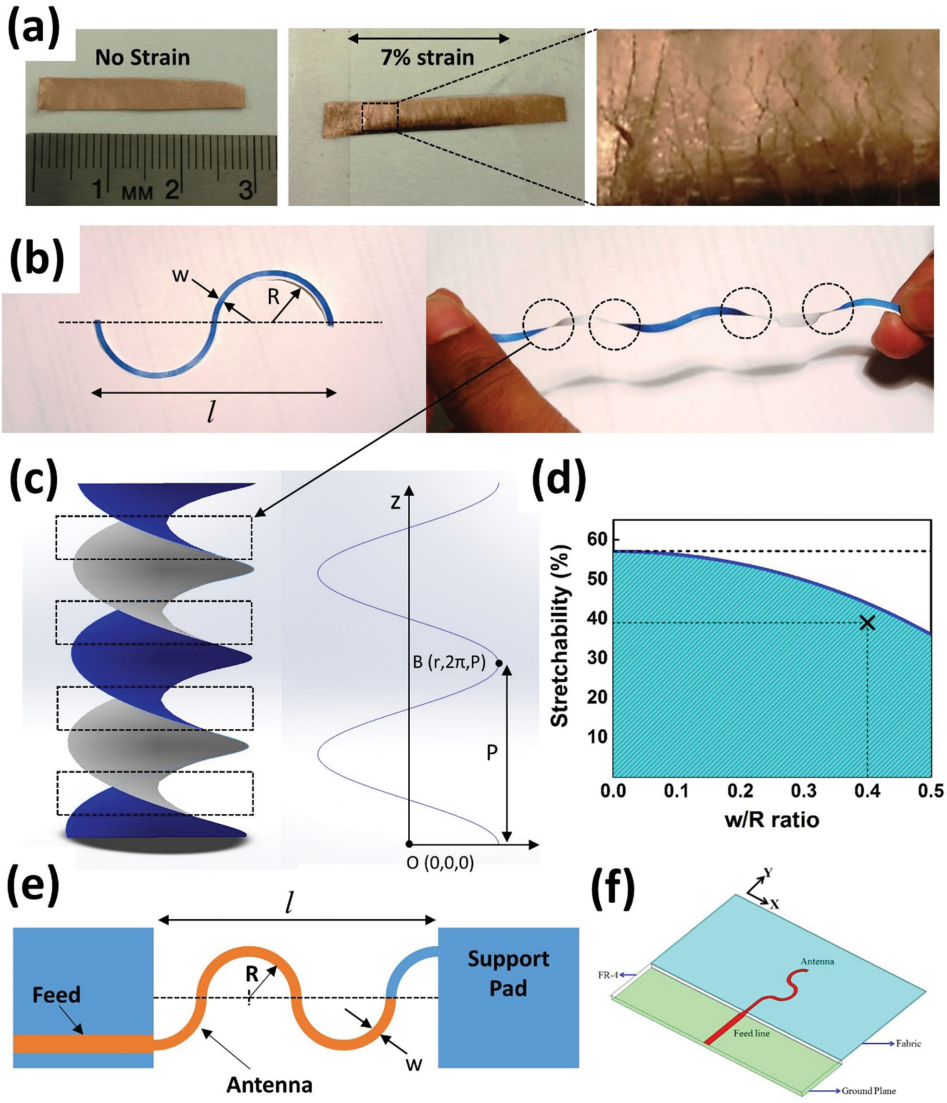

Figure 1. a) A strip of PDMS sputtered with 600 nm of copper gives a resistance of 6 Ω. When a strain of 7% is applied, the resistance goes out of the measuring range of the instrument (>20 MΩ) because of the development of cracks in the metal. b) A paper model representing the stretching behavior of a semicircular lateral spring. c) A 3D model illustrates that the original circumference of the spring makes an out-of-plane helical structure. d) Maximum stretchability by design as calculated using Equation (13). The "X" marks the value of stretchability experimentally obtained for the fabricated antennas. e) Design of the stretchable monopole antenna with feed and support structure. f) The simulation model used to define the stretchable antenna on fabric.

The stretchability is given by the ratio of the distance traveled by the 3D spiral in z-direction with the initial lateral length of the spring (l)

$$\varepsilon = \frac{nP}{2l} \tag{9}$$

$$\varepsilon = \frac{n}{2l}\sqrt{\left(\frac{2C}{n}\right)^2 - (\pi w)^2} \tag{10}$$

$$\varepsilon = \frac{1}{l}\sqrt{C^2 - \left(\frac{\pi n w}{2}\right)^2} \tag{11}$$

This generalized expression gives the maximum stretchability of a lateral spring due to its design. This analysis assumes that the materials involved are inherently unstretchable. If there is inherent stretching in the materials due to stress, it will be over and above the stretching calculated using this expression. From Equation (11), we can observe that if the width of the spring is very small, the equation simplifies to $\varepsilon = C/l$, as discussed in our previous work.[5] This is expected since a lateral spring with an infinitely small width can be approximated as a string that can stretch up to its original circumference. The addition of width necessitates the structure to twist which reduces the maximum stretchability. In case of the simple lateral spring shown in Figure 1b, the circumference is $2\pi R$ and the initial length, $l = 4R$, where R is the radius of the lobes of

© 2015 WILEY-VCH Verlag GmbH & Co. KGaA, Weinheim

the spring. Also, the number of twists is four as seen in the paper model. Hence, the stretchability in this case can be obtained as

$$\varepsilon = \frac{1}{4R}\sqrt{(2\pi R)^2 - \left(\frac{4\pi w}{2}\right)^2} \tag{12}$$

$$\varepsilon = \frac{\pi}{2}\sqrt{1 - \left(\frac{w}{R}\right)^2} \tag{13}$$

This simple equation describes the behavior of circular lateral springs made using inherently nonstretchable materials. It shows that the stretchability is only dependent on the ratio of the width of the spring and the radius of the lobes. This dependence is shown in Figure 1d. The maximum stretchability that can be obtained for a circular lateral spring design is 57.1%, when the width of the spring is negligible compared to its radius. Indeed, for the analysis to hold, the lateral springs need to twist out-of-plane. Hence, the width of the spring is generally less compared to the lobe radius. In case of the stretchable antennas fabricated in this work, the w/R ratio was 0.4, hence the maximum stretchability expected was 43% (Figure 1d). This maximum stretchability only applies in case of naturally unstretchable metals such as copper (Cu), tungsten (W), aluminum (Al), nickel (Ni). However, certain conductive materials, such as carbon (C), copper (Cu), and silver (Ag) nanowire dispersions and composites, have been shown to be inherently stretchable due to their structure.[31–37] This stretchability is over and above the one obtained by design as derived in this analysis. Hence, it can be added to the stretchability by design to obtain the total maximum stretchability. The stretchability can be further improved by pre-straining the design.[38–40]

3. Antenna Design

Based on this analysis, we designed the antenna in the form of a semicircular spring supported by two conducting polymer pads, as shown in Figure 1e. As previously discussed, when a force is applied along on the lateral direction, the spring structure twists at certain points, allowing the antenna to stretch. As a result, the length of the antenna does not physically increase during any point of stretching. The elongation is only obtained due to the restructuring of the lateral spring. This has two important consequences on the antenna performance. First, the metal does not crack since it is at no point under actual physical elongation. This helps maintaining the electrical performance of the metal. Second, the operation frequency of wire antennas is typically inversely proportional to their lengths. The geometry of the antenna also has some effect on the resonant frequency,[41] however in our case because we are using a simple monopole antenna which only stretches 30%, the effect of the changing geometry is not significant. In this work, we designed the monopole antenna to operate at 2.45 GHz for Wi-Fi applications (IEEE 802.11). This is an important frequency since it is one of the most commonly used Wi-Fi frequencies which can be a convenient option for data communication in wearable systems. The antenna was initially simulated in Ansys High Frequency Structure Simulator (HFSS) to optimize its length for the best impedance and radiation performance. These simulations showed that to work at 2.45 GHz the antenna length should be 30 mm which corresponds to quarter of a wavelength as is expected from a monopole antenna. The width of the antenna was kept at 1 mm, since releasing a larger structure without release holes would not have been possible in the fabrication phase. For radio frequency (RF) excitation, the antenna was connected to a microstrip feed line of 50 Ω impedance fabricated on FR-4 substrate. This rigid FR-4 substrate was used for testing purpose only. In reality, the antenna can be excited using an IC based driving circuit mounted on a flexible substrate.[15–17,42] This value of characteristic impedance was used since it is a standard for most of the RF measurement instruments.

After connecting the antenna to the feed line, it was initially simulated in air to observe its impedance and radiation performance. Once the optimization in air was complete, it was simulated with a flexible and stretchable textile fabric underneath as shown in Figure 1f. This was done since the proposed flexible and stretchable communication system would be integrated on human clothing. The thickness of this fabric was around 300 μm and its dielectric constant was measured to be 1.4. Using these properties of the fabric, it was observed that the antenna performance does not vary from the original design when it is simulated with the fabric underneath. With all the dimensions discussed above, we proceeded with the fabrication of the antenna. The simulated optimized performance of the antenna will be discussed with the measured results.

4. Fabrication Process

The process flow to fabricate the antenna is schematically represented in **Figure 2**a. We started with oxidized 4″ silicon wafers and deposited 1 μm amorphous silicon (a-Si) as sacrificial layer. The wafer was then spun with 4–μm–thick polyimide. The polyimide was patterned using aluminum hard mask (200 nm) and O_2 plasma. A seed layer for copper growth was then deposited on the wafer, followed by selective copper electroplating (4 μm). The seed layer was then removed by reactive ion etching (RIE) and the sacrificial layer was etched isotropically using XeF_2 to release the antenna structure. Figure 2b shows an optical image and the top-view and cross-section scanning electron microscopy (SEM) images for the fabricated antenna. The top view SEM images have been taken for the stretched antenna showing that the metal surface has no cracks due to stretching. The middle image shows the antenna twisting at the apex point. The cross-section SEM shows the metal layer grown on top of the polymer.

Since this antenna was designed for wearable electronics applications, its performance when attached to a fabric was crucial. We characterized the antennas stretching, flexing, mechanical properties and electrical characteristics all while it was attached to a stretchable fabric (typically used in Spandex). This was done to showcase the use of the stretchable antenna to monitor and communicate body movements and vital signs while being worn. The elongation of the lateral spring antenna is shown in **Figure 3**a. The antenna on fabric can be

© 2015 WILEY-VCH Verlag GmbH & Co. KGaA, Weinheim

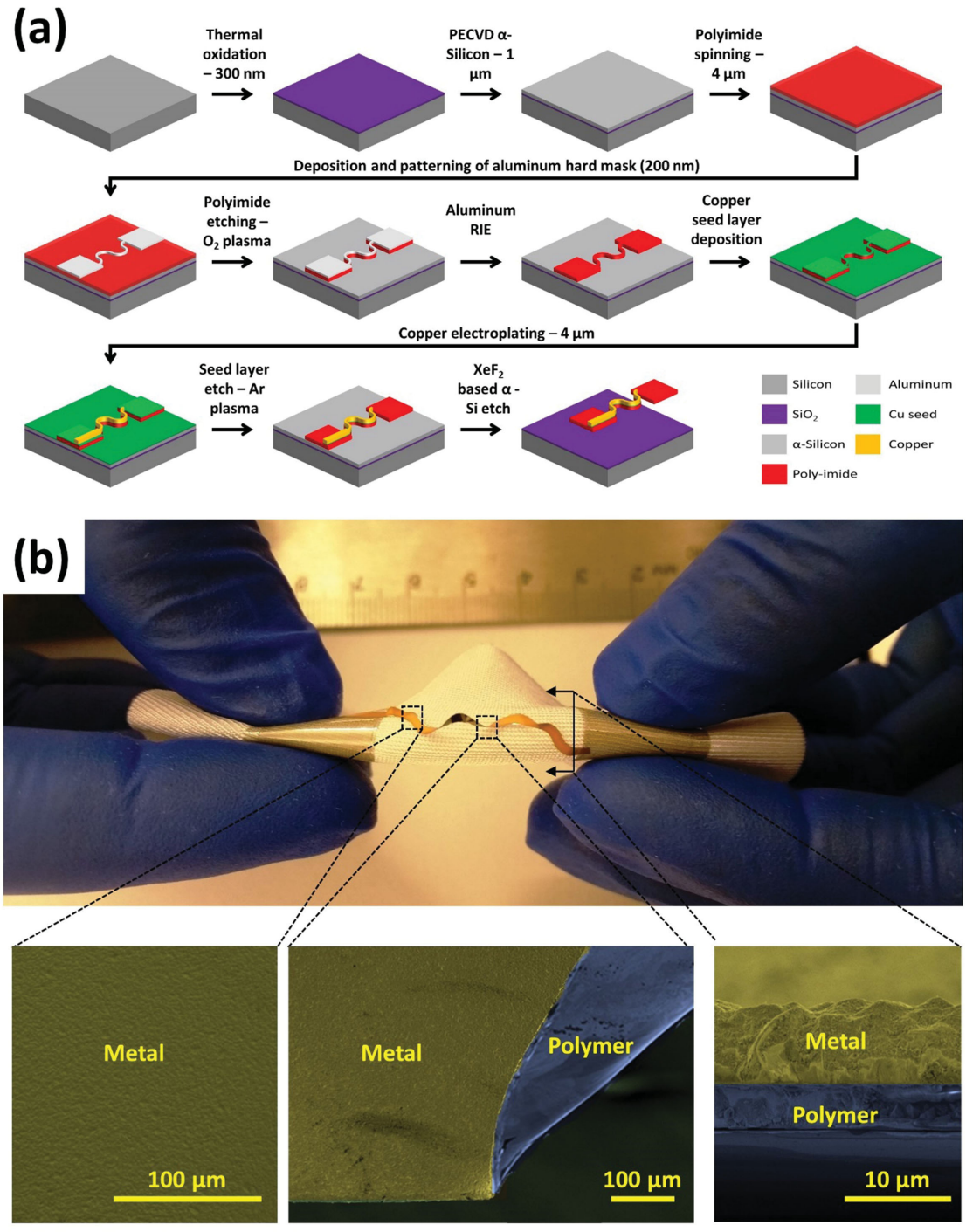

Figure 2. a) The schematic process flow for fabrication of stretchable antennas. b) Optical and scanning electron microscopy (SEM) images for the fabricated antenna show the top surface of the metal does not crack even when it is strained up to 30%.

flexed, twisted, stretched, and crumpled (Figure 3b). Further, the antenna can be attached on top of a sports T-shirt (used by athletes) made of stretchable fabric, and it will survive the stretching, flexing, and twisting associated with basic body movements (Figure 3c). As a result, the antenna can be connected to healthcare monitoring sensors on the body and the data can be wirelessly transmitted to a receiver such as a smart phone for storage or processing. This will allow athletes to measure parameters such as body temperature, oxygen saturation, and blood pressure in real-time during workouts. Further, healthcare professionals can use this technology to constantly monitor their patients' vital signs wirelessly. With the collection, processing, and storage of a large amount of data, this technology will allow big data analysis of healthcare data.

© 2015 WILEY-VCH Verlag GmbH & Co. KGaA, Weinheim

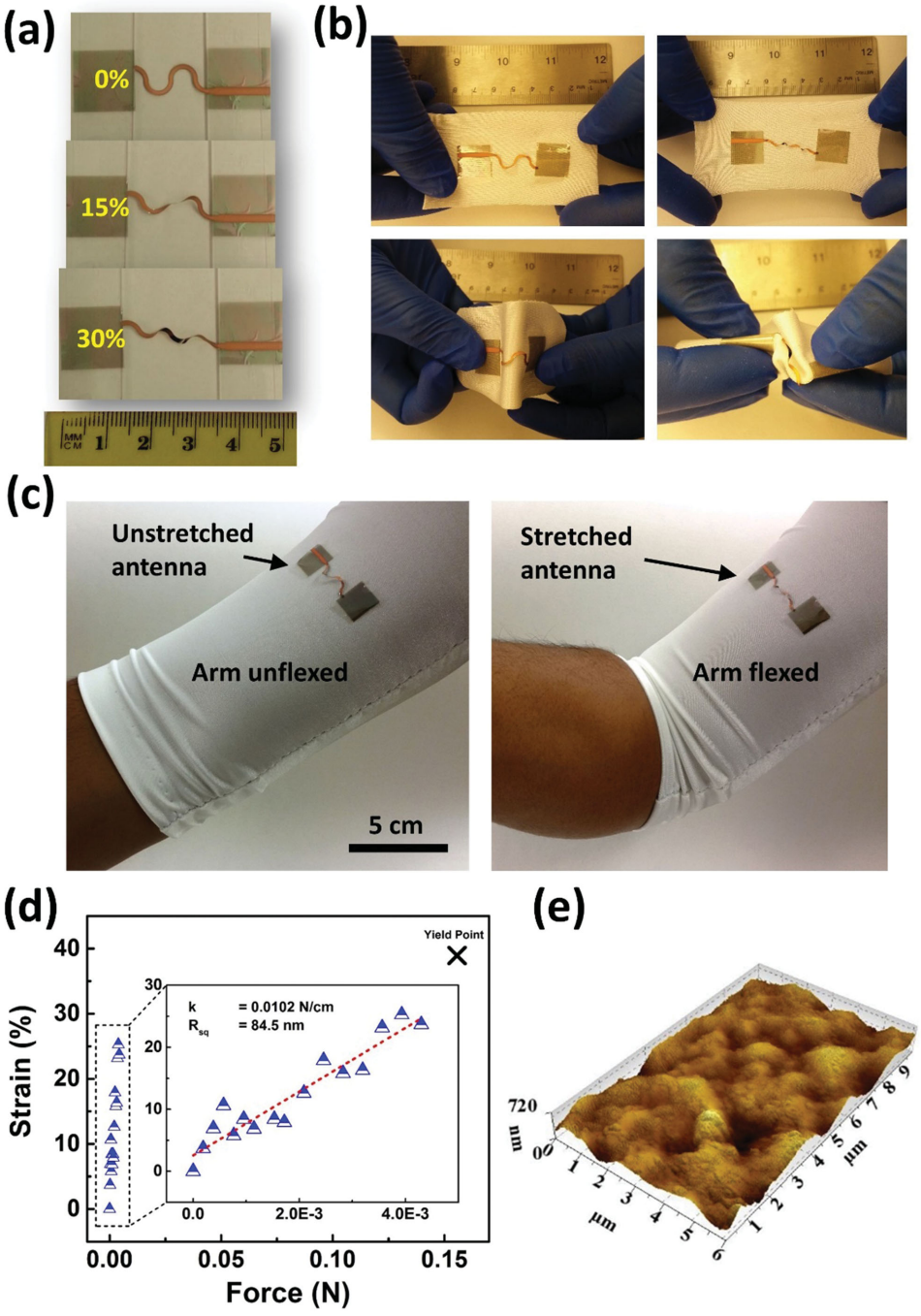

Figure 3. a,b) Optical images of the antenna-on-fabric show that it can be strained, bent, twisted and curled along with the fabric without physical damage. c) The antenna can be worn on the body and strained because of basic body movements. d) The stress–strain curve for the antenna shows that it behaves as a mechanical spring with a spring constant, $k = 0.01$ N cm^{-1}. The yield point for the antenna is reported as 0.155 N. e) The surface morphology for the electroplated copper obtained using atomic force microscopy (AFM). The RMS surface roughness was obtained as 84.5 nm.

5. Results and Discussion

The mechanical performance of the antenna (without fabric) is shown in Figure 3d. We report the maximum elongation for the antenna to be 39%. This is very close to the theoretical prediction of 43% obtained from the analysis. At this maximum elongation, the yield force was observed to be 0.15 N (15 MPa). However, the elastic limit for the antenna was around 30%. The antenna has enough mechanical strength to be handled manually without the need of any support structure. For further strengthening, the antenna can be packaged using a foam cavity structure to provide adequate space above and below the

© 2015 WILEY-VCH Verlag GmbH & Co. KGaA, Weinheim

antenna plane for out-of-plane twisting. The stress–strain curve obtained for the antenna in the elastic region is elaborated in the inset. Based on the linear fit for the measured points, the spring constant for the lateral springs was calculated to be 0.0102 N cm^{-1}. The copper layer was grown on polymer using electroplating, which generally leads to a rough thin film surface. The surface roughness of the as-grown copper thin film was evaluated using atomic force microscopy (AFM). The RMS surface roughness for the grown copper film was found to be 84.5 nm (Figure 3e).

Once the antenna is fabricated, it was characterized for its impedance and radiation performance. For RF excitation, an SMA (SubMiniature version A) connector was then soldered onto the substrate, such that its pin makes a contact with the

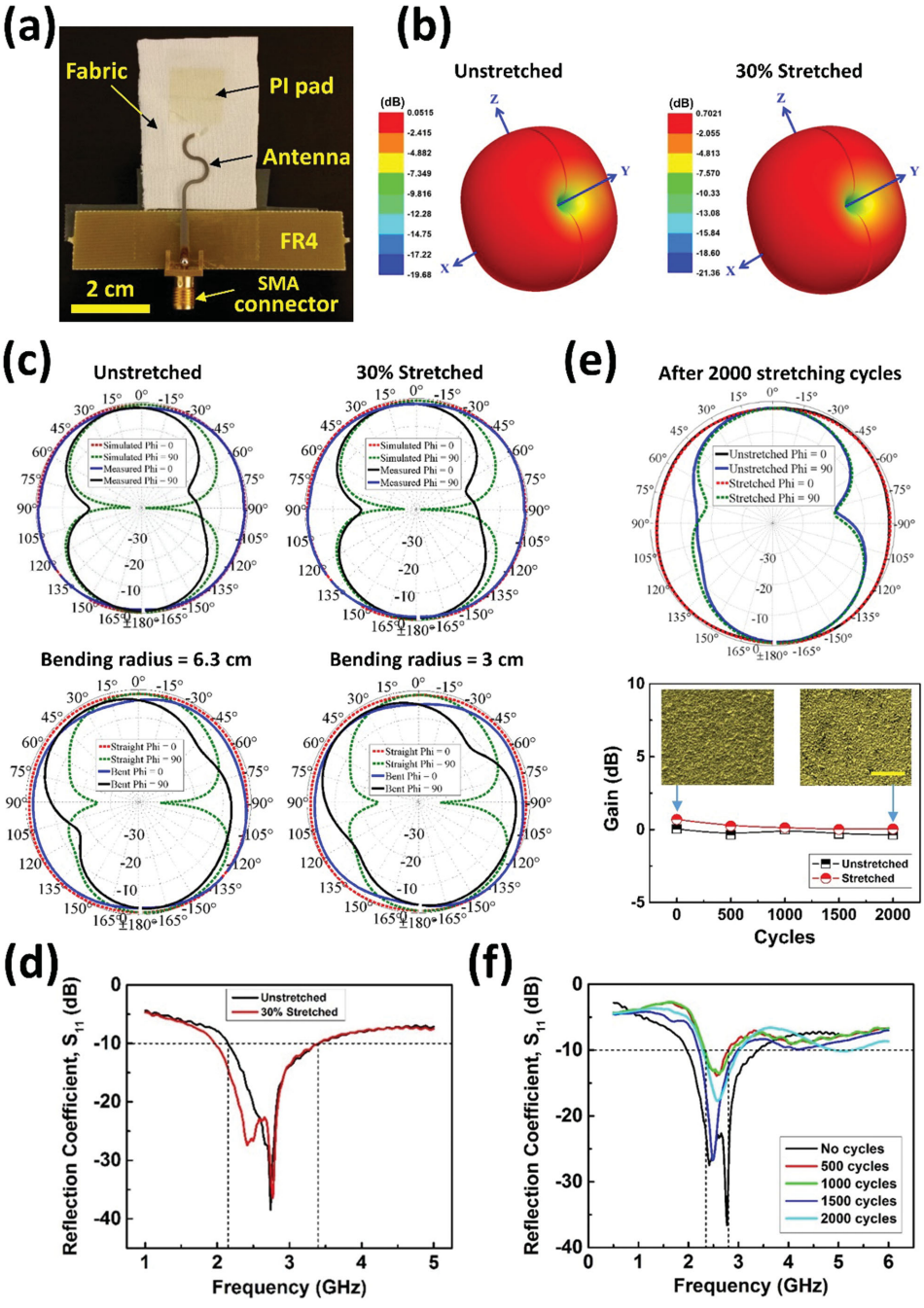

Figure 4. a) Optical image of stretchable antenna on fabric with FR-4 and SMA connector attached. b) The 3D radiation patterns for unstretched and stretched antennas show no significant change. c,d) The directionality, frequency, and bandwidth remain constant with the application of strain and bending. e) The stretchable antenna provides consistent performance over 2000 cycles of 30% strain. Bottom inset: Top view SEM images of the antenna before and after 2000 stretch cycles at 20% strain. Scale bar is 40 μm. f) The operation frequency and bandwidth (S_{11} < –10 dB at 2.45 GHz) are unchanged for 2000 cycles of strain.

© 2015 WILEY-VCH Verlag GmbH & Co. KGaA, Weinheim

feed line while the body of the connector was grounded. It was important to characterize the electrical properties of the antenna while attached to a piece of cloth. This was essential since the final communication system is proposed to be wearable and integrated onto textile fabrics. To this effect, the antenna was taped to a stretchable fabric to characterize the antenna in its presence. Hence, the effect of the cloth on the antenna performance is built into the results presented in this work. The final assembly is shown in **Figure 4**a.

The antenna was measured for its impedance performance using an Agilent's PNA (Performance Network Analyzer) N5232A, while the radiation pattern of the antenna was measured using Satimo's Star Lab (Anechoic Chamber). The measured 3D radiation patterns of Figure 4b demonstrated an omnidirectional behavior which is expected from a monopole antenna. The 2D polar plots of the radiation pattern show that there is a good agreement between the simulated and measured radiation performance (Figure 4c top). The H plane (XZ plane) of the antenna shows a constant gain in the complete elevation plane while the E plane (YZ plane) has nulls at $\theta = \pm 90°$, for both the cases i.e. stretched and unstretched. A measured gain of 0.05 dB was achieved from the antenna in the unstretched case which slightly changed to 0.7 dB in the stretched case.

Further, for the continuity of the communication channel, it is important that the operation frequency remains the same throughout its lifetime in any strain condition. To study this, the reflection coefficients (S_{11}) of the antenna at various strain values are plotted in Figure 4d. It can be observed that the antenna demonstrated a very good impedance matching for both the stretched and unstretched cases ($S_{11} < -10$ dB at 2.45 GHz). Also, the impedance bandwidth of the antenna was 51.1% and 53.4% for the unstretched and stretched case, respectively. Thus we report that the stretchable antenna retains all its essential properties on stretching, and can be effective in RF communication while being stretched. The other aspect studied for this antenna is the effect on its performance when it is bent. To do this, two cylinders of radii 6.3 and 3 cm were used for the antenna characterization. The cylinders were made using packing foam material which has a dielectric constant very close to air ($\varepsilon_r \approx 1$) and therefore will not affect the antenna characteristics. Figure 4c (bottom) shows the performance of the device under two different bending strains. It is clear that the radiation patterns have considerable similarity before and after the bending. Moreover the gain of the antenna remains preserved, independent of the bending radius. Hence, we can conclude that the antenna shows flexibility in addition to being stretchable.

For a robust wearable communication device, it is essential that the antenna survives several thousand cycles of strain. We tested the device for 2000 cycles for up to 30% strain. The polar plot of the radiation pattern of the antenna after cycling is shown in Figure 4e (top). It can be seen that there is no marked difference in the gain and radiation patterns from the initial unstretched case. The antenna, even after 2000 cycles of stretching, maintained an omnidirectional radiation pattern. The gain (Figure 4e bottom) of the device is retained over the strain cycles in addition to its radiation pattern. Furthermore, the reflection coefficient plot of Figure 4f illustrates that the operation frequency of the antenna remains unchanged for any number of stretching cycles. Top view scanning electron microscopy (SEM) images before and after 2000 strain cycles (Figure 4e bottom, inset) show that the copper thin film does not develop cracks due to straining. The SEMs were taken for 20% strained antennas. Further, the strain cycle test took a total of three weeks to complete. Hence, this test also shows that the copper antenna can survive in the ambient conditions for extended periods of time and retain its electrical properties during continued usage.

6. Far-Field Communication

Since the loading of the antenna by human tissue could increase the losses and cause a shift in the resonant frequency of the antenna, it was important to investigate the performance of the antenna under practical application conditions. We mounted the antenna on the arm of a consenting human subject using double sided Scotch tape (**Figure 5**a), to emulate the exact condition of application of the wearable antenna. A piece of cloth was kept as an intermediate layer between the antenna and the human body, as would be the case for the end user. The reflection coefficient of the antenna was measured for this scenario showing good match at 2.45 GHz (shown in Figure 5b). To measure the radiation pattern of the antenna mounted on the human arm two identical transceivers, Smart RF05 of Texas instrument, were used. The board contains CC2530 transceiver chip, which was programmed to work as a transmitter at 2.45 GHz on one board while the chip on the other board was programmed to operate as a receiver. The antenna under test was connected to the module working as the transmitter while the receiver module had a monopole antenna provided by the manufacturer connected to it. Using this set up, both H plane and E plane of the antenna were measured by rotating the receiver around the transmitter which was kept stationary at a point. A variation of 10 dB was observed in the power level received from the transmitter. This kind of variation is expected in an open environment due to the reflections from the surroundings present around the measurement area. These variations have been averaged out to plot them along with the radiation pattern of the antenna measured inside the anechoic chamber (Figure 5c). It can be seen that a good match has been obtained between the two measurements which shows that the antenna is suitable for wearable applications which is the target of this design.

Once the antenna had been measured for its impedance and radiation characteristics, we used it in a communication system operating at 2.45 GHz to carry out range measurements. For this purpose, two SmartRF05 evaluation boards of Texas Instruments were used as transmitter and receiver. The transmitter board was integrated with the stretchable antenna, while the receiver board had a simple monopole antenna integrated with it. The CC2530 chip provides a maximum transmitted RF power of 1 dBm (1.25 mW), while the receiver was programmed for –100 dBm sensitivity. This test was conducted in an open area on the university campus to simulate real life operating conditions (Supplementary video 1, Supporting Information). A plot showing the relationship between the received power and the distance between the transmitter and the receiver is shown in Figure 5d. The data points are the experimental values of power

© 2015 WILEY-VCH Verlag GmbH & Co. KGaA, Weinheim

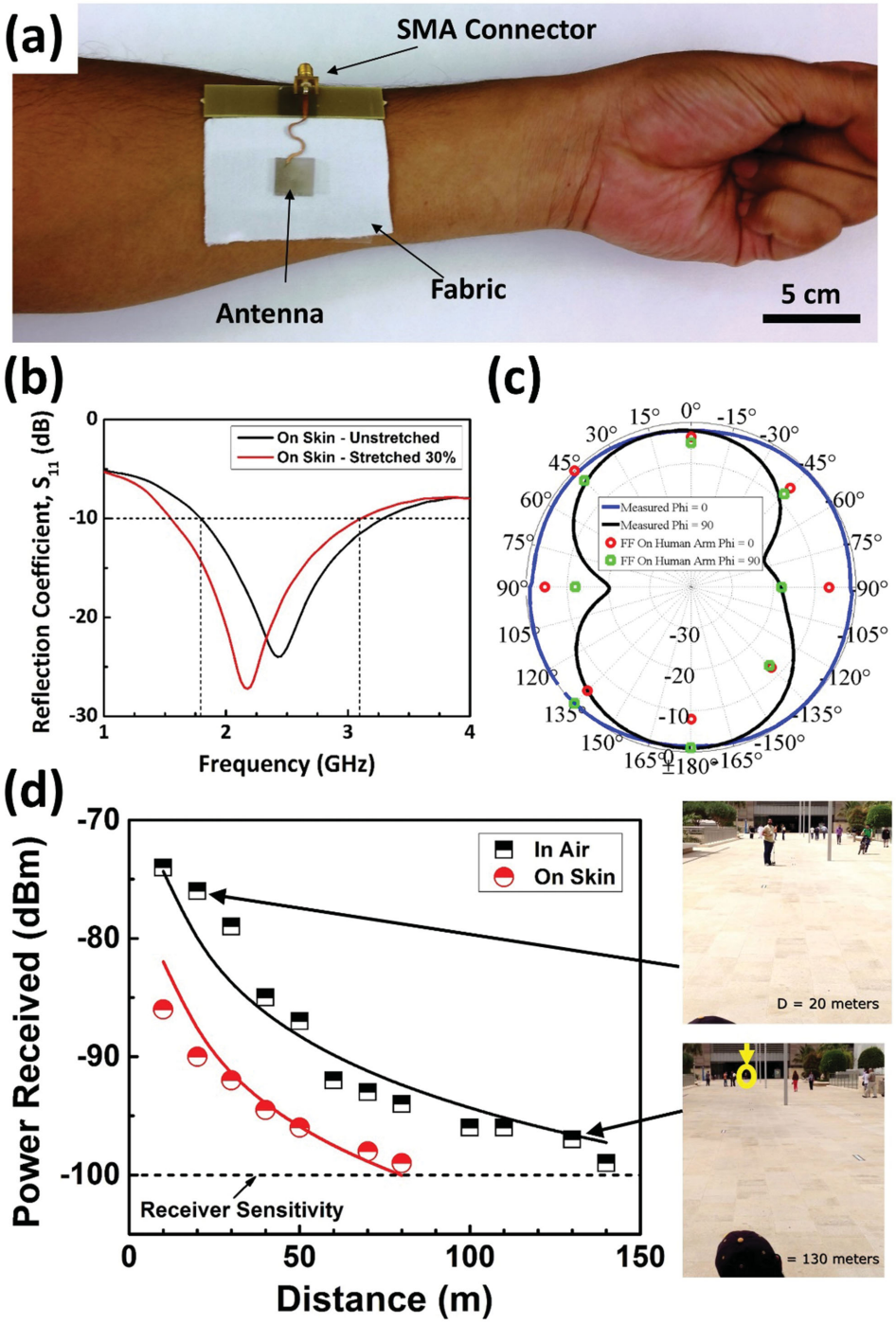

Figure 5. a) The antenna is mounted on a human arm, with a fabric as an intermediate layer, to simulate the final end user case. b,c) the S_{11} and radiation pattern are measured for the antenna on human arm to ascertain its performance in real application conditions. d) Far field communication test showing a plot showing the relationship between the received power and the distance between the transmitter and the receiver. The data points are the experimental values of power received by the receiver board, while the lines indicate the expected variation in received power versus distance according to Friis transmission equation.

received by the receiver board, while the lines indicate the expected variation in received power versus distance according to Friis transmission equation.[43] From this set up, it can be seen that the transmitter can communicate well for a distance of up to 140 m (across one and half soccer fields) while being in the air. If the transmitted power is increased to 10 dBm (10 mW), which can be easily achieved in Wi-Fi transmitters as per IEEE Standard 802.11, then the maximum range

© 2015 WILEY-VCH Verlag GmbH & Co. KGaA, Weinheim

can be increased to 394 m. As the final step the same range measurements were done with the proposed antenna design mounted on a human arm and connected to the transmitter while the receiver set up was the same. It was observed that when the antenna was mounted on the human arm the maximum distance or range values reduced to 80 m which is still good for the targeted applications. Again, if the transmitter power can be increased to 10 dBm then this range value would go up to 225 m for the antenna mounted on a human body. For all these measurements, the receiver sensitivity was kept constant at –100 dBm.

7. Conclusion

In conclusion, we present, for the first time, a comprehensive analysis of a flexible and stretchable copper antenna for far-field communication (up to 80 m while mounted on a stretchable fabric and worn by a human subject), which maintains its properties during stretching, bending and strain cycles. The antenna is designed using a metal/polymer thin film bilayer and lateral spring structure. Copper is used for fabrication of the antenna since it is a common, low-cost, CMOS compatible metal. We report the gain for the fabricated antenna as close to 0 dB for both stretched and unstretched cases, and after 2000 stretching cycles. The antenna retains all its essential properties such as gain, radiation pattern, directionality, operation frequency and bandwidth for up to 30% strain and for 2000 cycles of strain. The antenna communicates in the 2.45 GHz Wi-Fi band under any strain condition (up to 30%), thus paving way for wearable electronics to communicate data reliably over a long range. In real life operating conditions, the antenna on human arm communicates up to a distance of 80 m with 1.25 mW transmitted power.

8. Experimental Section

Copper/PDMS Strip: A 10:1 mixture of base and curer (Sylgard 184 Silicone Elastomer Kit, Dow Corning) was made in a plastic beaker and spun on a wafer at 500 rpm. The PDMS was cured at 100 °C for 20 min before deposition of 600 nm of copper using argon plasma sputtering (25 sccm, 5 mTorr, 400 W). The PDMS was removed from the substrate and cut into a strip to perform the experiment.

Stretchable Antennas: The fabrication process for the stretchable antennas started with 4″ silicon wafers thermally oxidized using a dry-wet-dry oxidation cycle to obtain 300 nm of SiO_2. A 1 μm layer of amorphous silicon was deposited using plasma enhanced chemical vapor deposition (PECVD) at 250 °C for 25 min. This was followed by spinning 4 μm layer of polyimide (PI2611, HD Microsystems) at 4000 rpm for 60 s. The polyimide (PI) was cured first at 90 °C for 90 s, then at 150 °C for 90 s and finally at 350 °C for 30 min. A 200 nm layer of aluminum was deposited on top of PI as hard mask using argon plasma sputtering (25 sccm Ar, 5 mTorr, 400 W, 600 s). The aluminum was patterned using AZ1512 photoresist (40 mJ cm^{-2}) and etched using reactive ion etching (RIE) at 80 °C for 95 s. The PI was then etched using oxygen plasma (50 sccm O_2) at 60 °C for 16 min. A Cr/Au (20/200 nm) bilayer was deposited as a seed layer for copper electroplating using argon plasma sputtering. A Cr/Cu bilayer or any other metal layer compatible with copper ECD can also be used as seed to reduce cost. The wafer was spun with photoresist AZ ECI 3027 at 1750 rpm for 30 s and was developed using AZ 726 MIF for 60 s to expose the area to be electroplated. The copper electroplating was done at 45 °C with 0.488 Amp current for 5 min to yield a 4 μm thick layer. The copper seed layer was then etched using argon plasma (30 sccm Ar, 150 W RF) for 3 min. Finally, the wafer was subjected to isotropic gas phase etching of amorphous silicon using XeF_2 for 60 cycles at 4 Torr to release the antenna.

Supporting Information

Supporting Information is available from the Wiley Online Library or from the author.

Acknowledgements

The authors acknowledge KAUST OCRF Grant CRG-1–2012-HUS-008.

Received: August 5, 2015
Revised: August 27, 2015
Published online: October 6, 2015

[1] D.-H. Kim, N. Lu, R. Ma, Y.-S. Kim, R.-H. Kim, S. Wang, J. Wu, S. M. Won, H. Tao, A. Islam, K. J. Yu, T.-I. Kim, R. Chowdhury, M. Ying, L. Xu, M. Li, H.-J. Chung, H. Keum, M. McCormick, P. Liu, Y.-W. Zhang, F. G. Omenetto, Y. Huang, T. Coleman, J. A. Rogers, *Science* **2011**, *333*, 838.
[2] J. Kim, A. Banks, H. Cheng, Z. Xie, S. Xu, K.-I. Jang, J. W. Lee, Z. Liu, P. Gutruf, X. Huang, P. Wei, F. Liu, K. Li, M. Dalal, R. Ghaffari, X. Feng, Y. Huang, S. Gupta, U. Paik, J. A. Rogers, *Small* **2015**, *11*, 906.
[3] W.-H. Yeo, Y.-S. Kim, J. Lee, A. Ameen, L. Shi, M. Li, S. Wang, R. Ma, S. H. Jin, Z. Kang, Y. Huang, J. A. Rogers, *Adv. Mater.* **2013**, *25*, 2773.
[4] Y. Zang, F. Zhang, C.-A. Di, D. Zhu, *Mater. Horiz.* **2015**, *2*, 140.
[5] A. M. Hussain, E. B. Lizardo, G. A. Torres Sevilla, J. M. Nassar, M. M. Hussain, *Adv. Healthcare Mater.* **2015**, *4*, 665.
[6] J. A. Fan, W.-H. Yeo, Y. Su, Y. Hattori, W. Lee, S.-Y. Jung, Y. Zhang, Z. Liu, H. Cheng, L. Falgout, M. Bajema, T. Coleman, D. Gregoire, R. J. Larsen, Y. Huang, J. A. Rogers, *Nat. Commun.* **2014**, *5*, 3266.
[7] M. Kaltenbrunner, T. Sekitani, J. Reeder, T. Yokota, K. Kuribara, T. Tokuhara, M. Drack, R. Schwodiauer, I. Graz, S. Bauer-Gogonea, S. Bauer, T. Someya, *Nature* **2013**, *499*, 458.
[8] T. Someya, Y. Kato, T. Sekitani, S. Iba, Y. Noguchi, Y. Murase, H. Kawaguchi, T. Sakurai, *Proc. Natl. Acad. Sci. USA* **2005**, *102*, 12321.
[9] T. Someya, T. Sakurai, in *Organic Electronics*, Wiley-VCH, Weinheim, Germany **2006**, p. 395.
[10] T. Someya, T. Sekitani, S. Iba, Y. Kato, H. Kawaguchi, T. Sakurai, *Proc. Natl. Acad. Sci. USA* **2004**, *101*, 9966.
[11] D.-H. Kim, N. Lu, R. Ghaffari, Y.-S. Kim, S. P. Lee, L. Xu, J. Wu, R.-H. Kim, J. Song, Z. Liu, J. Viventi, B. de Graff, B. Elolampi, M. Mansour, M. J. Slepian, S. Hwang, J. D. Moss, S.-M. Won, Y. Huang, B. Litt, J. A. Rogers, *Nat. Mater.* **2011**, *10*, 316.
[12] D. Son, J. Lee, S. Qiao, R. Ghaffari, J. Kim, J. E. Lee, C. Song, S. J. Kim, D. J. Lee, S. W. Jun, S. Yang, M. Park, J. Shin, K. Do, M. Lee, K. Kang, C. S. Hwang, N. Lu, T. Hyeon, D.-H. Kim, *Nat. Nano.* **2014**, *9*, 397.
[13] J. J. S. Norton, D. S. Lee, J. W. Lee, W. Lee, O. Kwon, P. Won, S.-Y. Jung, H. Cheng, J.-W. Jeong, A. Akce, S. Umunna, I. Na, Y. H. Kwon, X.-Q. Wang, Z. Liu, U. Paik, Y. Huang, T. Bretl, W.-H. Yeo, J. A. Rogers, *Proc. Natl. Acad. Sci. USA* **2015**, *112*, 3920.

© 2015 WILEY-VCH Verlag GmbH & Co. KGaA, Weinheim

[14] J. P. Rojas, A. Arevalo, I. G. Foulds, M. M. Hussain, *Appl. Phys. Lett.* **2014**, *105*, 154101.
[15] J. P. Rojas, G. A. Torres Sevilla, M. T. Ghoneim, S. B. Inayat, S. M. Ahmed, A. M. Hussain, M. M. Hussain, *ACS Nano* **2014**, *8*, 1468.
[16] G. A. T. Sevilla, J. P. Rojas, H. M. Fahad, A. M. Hussain, R. Ghanem, C. E. Smith, M. M. Hussain, *Adv. Mater.* **2014**, *26*, 2794.
[17] G. A. Torres Sevilla, M. T. Ghoneim, H. Fahad, J. P. Rojas, A. M. Hussain, M. M. Hussain, *ACS Nano* **2014**, *8*, 9850.
[18] C. Shi, W. Zhigang, P. Hallbjorner, K. Hjort, A. Rydberg, *IEEE Trans. Antennas Propag.* **2009**, *57*, 3765.
[19] J.-H. So, J. Thelen, A. Qusba, G. J. Hayes, G. Lazzi, M. D. Dickey, *Adv. Funct. Mater.* **2009**, *19*, 3632.
[20] M. Kubo, X. Li, C. Kim, M. Hashimoto, B. J. Wiley, D. Ham, G. M. Whitesides, *Adv. Mater.* **2010**, *22*, 2749.
[21] L. Song, A. C. Myers, J. J. Adams, Y. Zhu, *ACS Appl. Mater. Interfaces* **2014**, *6*, 4248.
[22] A. Arriola, J. I. Sancho, S. Brebels, M. Gonzalez, W. D. Raedt, *IET Microwaves Trans. Antennas Propag* **2011**, *5*, 852.
[23] M. J. Makin, F. J. Minter, *Acta Metall.* **1960**, *8*, 691.
[24] H. Yung-Yu, P. Cole, L. Daniel, W. Xianyan, R. Milan, Z. Baosheng, G. Roozbeh, *J. Micromech. Microeng.* **2014**, *24*, 095014.
[25] H. Yung-Yu, M. Gonzalez, F. Bossuyt, J. Vanfleteren, I. De Wolf, *IEEE Trans. Electron Devices* **2011**, *58*, 2680.
[26] S. P. Lacour, J. Jones, S. Wagner, T. Li, Z. Suo, *Proc. IEEE* **2005**, *93*, 1459.
[27] Y. Zhang, H. Fu, S. Xu, J. A. Fan, K.-C. Hwang, J. Jiang, J. A. Rogers, Y. Huang, *J. Mech. Phys. Solids* **2014**, *72*, 115.
[28] C. Lv, H. Yu, H. Jiang, *Extreme Mech. Lett.* **2014**, *1*, 29.
[29] S. Xu, Y. Zhang, J. Cho, J. Lee, X. Huang, L. Jia, J. A. Fan, Y. Su, J. Su, H. Zhang, H. Cheng, B. Lu, C. Yu, C. Chuang, T.-I. Kim, T. Song, K. Shigeta, S. Kang, C. Dagdeviren, I. Petrov, P. V. Braun, Y. Huang, U. Paik, J. A. Rogers, *Nat. Commun.* **2013**, *4*, 1543.
[30] Y. M. Song, Y. Xie, V. Malyarchuk, J. Xiao, I. Jung, K.-J. Choi, Z. Liu, H. Park, C. Lu, R.-H. Kim, R. Li, K. B. Crozier, Y. Huang, J. A. Rogers, *Nature* **2013**, *497*, 95.
[31] W. Ju Yeon, K. Kyun Kyu, L. Jongsoo, K. Ju Tae, H. Chang-Soo, *Nanotechnology* **2014**, *25*, 285203.
[32] H.-W. Cui, K. Suganuma, H. Uchida, *Nano Res.* **2015**, 1.
[33] Y. Cheng, S. Wang, R. Wang, J. Sun, L. Gao, *J. Mater. Chem. C* **2014**, *2*, 5309.
[34] F. Xu, Y. Zhu, *Adv. Mater.* **2012**, *24*, 5117.
[35] J. Song, J. Li, J. Xu, H. Zeng, *Nano Lett.* **2014**, *14*, 6298.
[36] Y. Won, A. Kim, W. Yang, S. Jeong, J. Moon, *NPG Asia Mater.* **2014**, *6*, e132.
[37] M.-S. Lee, J. Kim, J. Park, J.-U. Park, *Nanoscale Res. Lett.* **2015**, *10*, 1.
[38] F. Xu, X. Wang, Y. Zhu, Y. Zhu, *Adv. Funct. Mater.* **2012**, *22*, 1279.
[39] X. Wang, H. Hu, Y. Shen, X. Zhou, Z. Zheng, *Adv. Mater.* **2011**, *23*, 3090.
[40] M. Zu, Q. Li, G. Wang, J.-H. Byun, T.-W. Chou, *Adv. Funct. Mater.* **2013**, *23*, 789.
[41] D. G. Fang, *Antenna Theory and Microstrip Antennas*, CRC Press, Boca Raton, Florida, USA, **2009**, p. 3.
[42] Y. Xu, *IEEE Sens. J.* **2013**, *13*, 3962.
[43] C. A. Balanis, *Antenna Theory: Analysis and Design*, John Wiley & Sons, Hoboken, NJ, USA **2012**.

© 2015 WILEY-VCH Verlag GmbH & Co. KGaA, Weinheim